



Spatial distribution, pollution characteristics and risk assessment of heavy metals in soils: A case study in the desert city of India

Leela Kaur*, Divyaman Singh Rathore, Rajaram Choyal

¹Department of Environmental Science, Maharaja Ganga Singh University, Bikaner, Rajasthan, India

* Corresponding author E.mail: leela.kaur@gmail.com

Article info

Received 17/7/2025; received in revised form 13/10/2025; accepted 10/1/2026

DOI: [10.60923/issn.2281-4485/22454](https://doi.org/10.60923/issn.2281-4485/22454)

© 2026 The Authors.

Abstract

The study aims to assess the accumulation of ten heavy metals (As, Cd, Cr, Co, Cu, Fe, Mn, Ni, Pb, and Zn) in soils of the desert city of Rajasthan. Heavy metals analysis in industrial soils was assessed by following standard methods for two consecutive years. Principal component analysis (PCA), correlation matrix, spatial distribution, contamination factor (CF), degree of contamination (CD), pollution load index (PLI) and potential ecological risk index (PERI) in soil and plants were assessed to find out the metal contamination level. Furthermore, this study also conducted human health risk assessment for adults and children by using the health risk assessment model recommended by the United States Environmental Protection Agency (USEPA). The highest concentration of heavy metals such as As (7.74 mg/kg), Cu (18.22 mg/kg), Fe (2981 mg/kg), Ni (25.11 mg/kg), and Zn (106.12) in Rani Bazar, Co (5.54 mg/kg) and Pb (13.86 mg/kg) in Bichhwal and Cr (14.32 mg/kg) and Mn (71.8 mg/kg) in Khara in 2019. Whereas, Cd (4.50 mg/kg) was maximum in Karni industrial soil in 2020. Whereas, the high metal content in plants was observed mainly in 2020 such as As (30.9 mg/kg) and Zn (376.7 mg/kg) in *Abutilon indicum*, Cd (29.93 mg/kg) in *Calotropis procera*, Cr (341.6 mg/kg), Cu (400.61 mg/kg) and Ni (301.99 mg/kg) in *Aerva pseudotomentosa*, Fe (14496 mg/kg) and Mn (1319.89 mg/kg) in *Cicer arietinum*, Pb (976.7 mg/kg) in *Coriandrum sativum*. Though only *Citrullus colocynthis* contain high concentration of Co (11.96 mg/kg) in 2019. Plant species show hyperaccumulation towards As, Cd, Cr, Cu, Co, Fe, Mn, Ni, Pb, and Zn with more than 1 values of bioconcentration factor and translocation factor specifying their effectiveness in uptake and transfer of more than one element from soil to shoot. The non-carcinogenic health risk assessment shows that HQ values for heavy metals such as As, Cd, Cr, Cu, Fe, Ni, Mn, Pb in plants were above the recommended guideline level. In carcinogenic risk assessment, CRI in adult group of Rani Bazar industrial soil in 2019 were found at high cancer risk. Moreover, selected plants also show cancer risk for As, Cd, Cr, Ni and Pb metals. Therefore, consumption of plants may produce cancer risk in humans too. Henceforth, monitoring and management of heavy metals is advocated to avert the metal health hazards to humans. The study can be utilized as baseline for further human health risk assessment of heavy metals.

Keywords: Industrial soil; heavy metals; metal pollution; desert plants; health risk assessment.

Introduction

Industrial expansion and intensive agricultural practices have significantly escalated environmental pollution, particularly through the release of heavy metals into soil, water, and air (Adnan et al., 2024). These toxic elements, originating from both natural sources

like volcanic activity and anthropogenic activities such as mining, fertilizer use, and industrial effluent discharge, pose serious threats to ecosystems and human health (Yang et al., 2018; Zaynab et al., 2020; Cui et al., 2022). Metals, such as lead (Pb), cadmium (Cd), mercury (Hg), and arsenic (As), are non-biodegrada-

ble and tend to accumulate in ecosystems, posing long-term risks to both ecological and human health (Sharma and Nagpal, 2018; Ali et al., 2019). In India, urban areas face acute challenges due to industrial effluent discharge which has rendered local water bodies ecologically degraded (Singh and Yadav, 2014). The persistence of heavy metals in soil not only disrupts microbial communities and nutrient cycles but also impairs plant growth and productivity (Ayangbenro and Babalola, 2017; Bakshi et al., 2018). To mitigate these impacts, phytoremediation using native plant species offers a sustainable and cost-effective solution, with species like *Prosopis juliflora* and *Brassica juncea* showing promising metal uptake capabilities (Usman et al., 2019; Kafle et al., 2022). The dual benefit of pollution mitigation and carbon sequestration underscores the importance of evaluating these plants for large-scale environmental restoration (Tanwar et al., 2019; Kunwar and Jain, 2022). Bikaner's industrial landscape (northwestern region of Rajasthan) comprises four major zones i.e., Rani Bazar, Bichhwal, Karni, and Khara, each hosting a diverse array of small scale and medium scale industries. These include food processing units (such as snacks locally named namkeen, bhujia, papad), woolen mills, agro-based enterprises (e.g., flour mills, edible oil, guar gum), ceramic manufacturers, and mineral-based industries such as gypsum grinding and plaster of Paris production.

While these industries contribute to regional economic development, they also generate substantial industrial discharge, often containing heavy metals and chemical residues. Effluents from wool processing, ceramic glazing, and mineral grinding are known to release pollutants like chromium, lead, and cadmium into nearby soil and water bodies (Adediran et al., 2021). The lack of adequate treatment facilities and proximity of these zones to residential and agricultural areas, especially in Bichhwal and Khara, exacerbates the risk of environmental contamination and public health hazards. This underscores the urgent need for systematic monitoring and sustainable remediation strategies tailored to the industrial profile of Bikaner. This study aims to assess heavy metal contamination in the soils of the Bikaner's industrial zones, evaluate the phytoremediation potential of local flora, and map spatial distribution using geospatial tools, ultimately contributing to environmental restoration and public health protection.

Methodology

Study area and site selection

Bikaner city lies in the north-western region of Rajasthan, within the expansive Thar Desert, which spans parts of Rajasthan, Gujarat, Haryana, and Punjab (Fig.1).

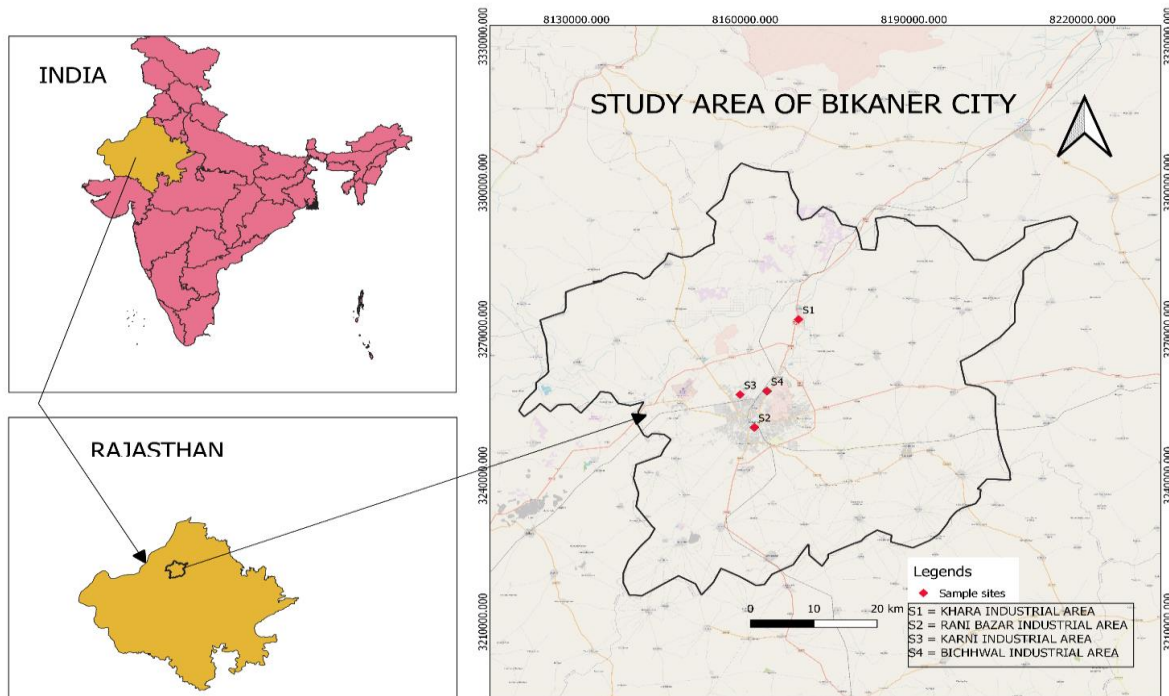


Figure 1. Study area map

The soil surrounding Bikaner is predominantly arid and sandy, characterized by sparse vegetation. Geographically, the district covers approximately 30,247.90 km² and is situated between latitudes 27°11' to 29°03' N and longitudes 71°54' to 74°12' E. The city stands at an average elevation of 237 meters above sea level. Climatic conditions are extreme, with summer temperatures exceeding 45°C and winter lows dropping below 0°C. Annual rainfall ranges from 260 to 440 mm, and the landscape is largely flat. Due to its desert climate, vegetation in and around Bikaner is limited to drought-resistant species. Common crops cultivated include wheat, mustard, groundnut, and various millets. Dominant tree species in the region include

khejri (*Prosopis cineraria*), kikar (*Acacia nilotica*), rohida (*Tecomella undulata*), ber (*Ziziphus nummularia*), ker (*Capparis decidua*), and jaal (*Salvadora persica*), with occasional presence of shisham, pipal, babul, and siris. The local fauna comprises black buck, chinkara, fox, jackal, mongoose, scorpion, snake, striped squirrel, wild boar, and wolf. While the city lacks proximity to major rivers, small lakes and reservoirs serve as crucial water sources for agriculture and domestic use. Among these, Gajner Lake, located about 32 km southwest of Bikaner, is a prominent water body. For this study, four major industrial areas (Rani Bazar, Bichhwal, Karni, and Khara) were selected and their geographical locations is shown in Figure 1 and detailed in Table 1 .

Industrial Area	Latitude (Degree)	Longitude (Degree)	Elevation (m)	Area (Hectares)
Rani Bazar	28.05255	73.4779	235	70
Karni	28.0727	73.5455	225	86.82
Khara	28.0196	73.3906	225	294.18
Bichhwal	28.0101	73.3762	225	157

Table 1
Locations of the selected industrial areas of Bikaner City

Sampling and analytical procedures

Soil, and selected plant samples were collected from designated industrial zones in Bikaner City during two distinct periods: August–September 2019 and February 2020. Concurrently, climatic data including temperature, atmospheric pressure, humidity, precipitation, and wind speed were recorded for both years to contextualize environmental conditions during sampling. In 2019, average temperatures in Bikaner were 32.68 °C in August and 32.92 °C in September, while February 2020 saw a significantly lower average of 18.08 °C. Atmospheric pressure measured 97.3 kPa and 97.8 kPa in August and September 2019, respectively, rising to 98.98 kPa in February 2020. Relative humidity was 57.38% in August and 52% in September 2019, dropping to 35.69% in February 2020. Precipitation occurred only in August 2019, averaging 5.27 mm/day. Wind speeds ranged from 3.6 m/s in August to 2.76 m/s in September 2019, with a slight increase to 2.95 m/s in February 2020.

Soil and plant analysis

Soil sampling was conducted at a depth of 5–15 cm, following the removal of surface debris to minimize contamination with the help of a spatula. Composite soil samples were then stored in labelled plastic contai-

ners for laboratory analysis. In the laboratory, samples were transferred to petri dishes and dried using a hot air oven. Whereas, plant specimens collected for analysis included bitter cucumber (*Citrullus colocynthis*), browntop millet (*Brachiaria ramosa*), watermelon (*Cucumis lanatus*), apple of sodom (*Calotropis procera*), wild gourd (*Cucumis prophetarum*), indian mallow (*Abutilon indicum*), bui (*Aerva pseudotomentosa*), jungle kikar (*Prosopis juliflora*), chickpeas (*Cicer arietinum*), jangi gobi (*Launaea procumbens*), spinach (*Spinacia oleracea*), and coriander (*Coriandrum sativum*) as shown in Figure 2. Each plant sample was separated into root, shoot, and leaf components, then dried in a hot air oven. A subsample of soil and of plant weighing between 0.5 g and 1.0 g was measured using a precision balance (Wensler Limited). Each sample was placed in a 250 ml beaker and digested with 12 ml of aqua regia (3:1 mixture of HCl and HNO₃). The beakers were covered with watch glasses and heated on a hot plate at 80 °C for 2 hours. After cooling, the digested samples were filtered through filter paper (Whatman) and diluted to a final volume of 100 ml. The filtrates were analyzed for selected heavy metals like As, Cd, Co, Cr, Cu, Fe, Mn, Ni, Pb, and Zn using inductively coupled plasma atomic emission spectrometry (ICP-E-9000, Shimadzu) for the first sampling, and inductively coupled plasma

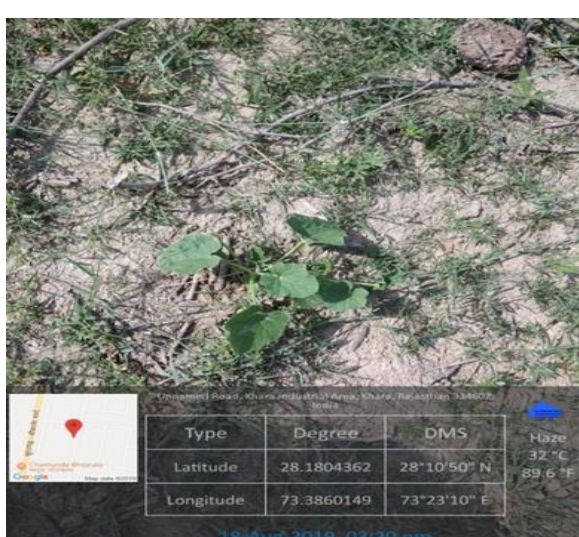
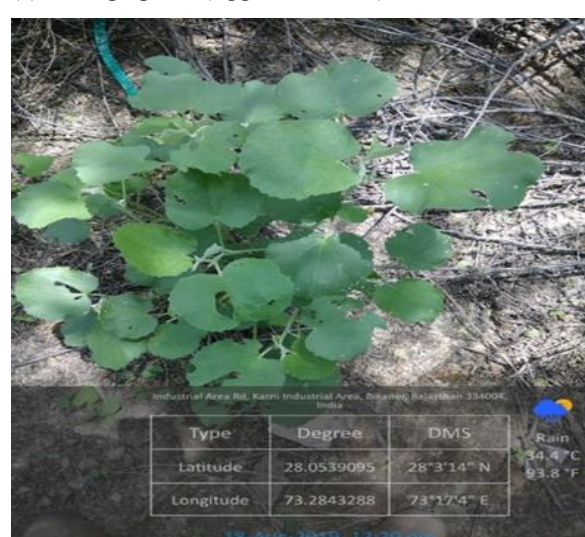
(a) *Aerva pseudotomentosa* (Bui)(b) *Citrullus colocynthis* (Bitter cucumber)(c) *Brachiaria ramosa* (Browntop millet)(d) *Calotropis procera* (Apple of sodom)(e) *Cucumis prophetarum* (Wild gourd)(f) *Abutilon indicum* (Indian mallow)

Figure 2. Selected plant samples (a-f) of the study area.

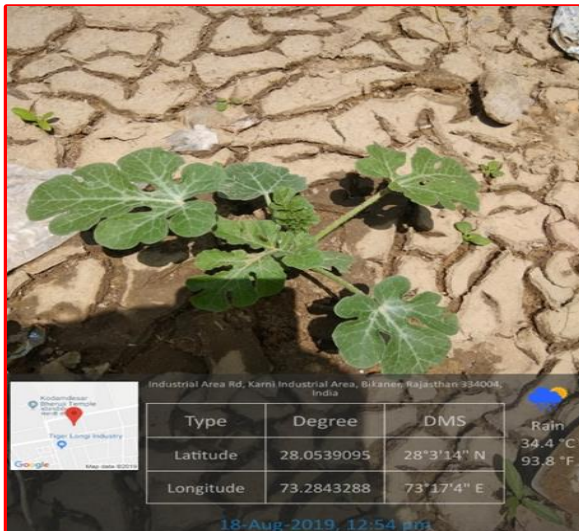
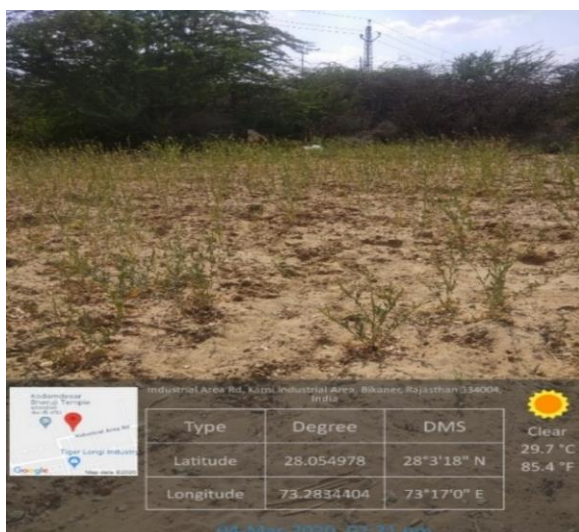
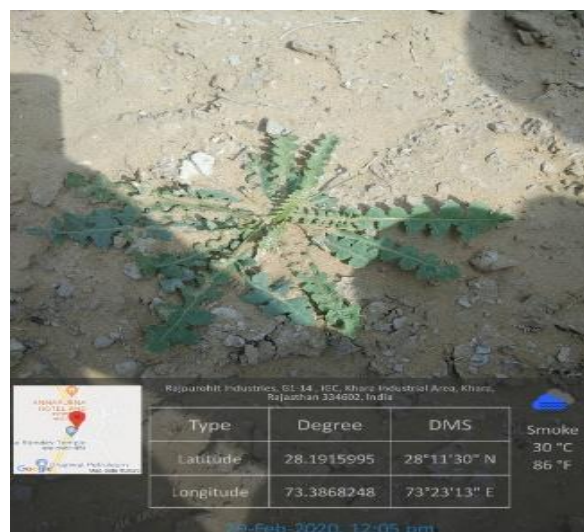
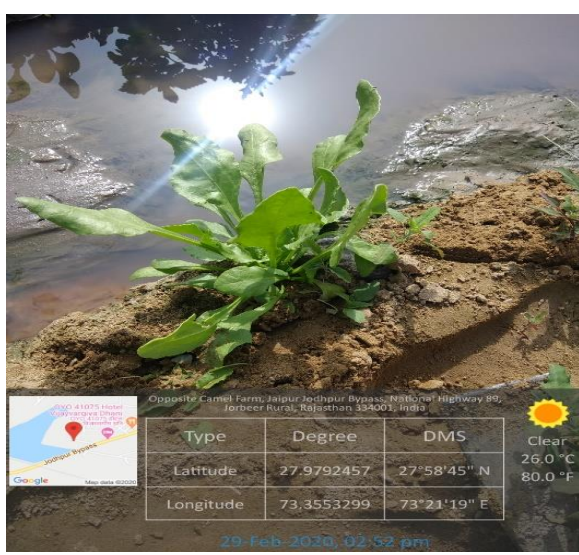
(g) *Cucumis lanatus* (Watermelon)(h) *Prosopis juliflora* (Jungle kikar)(i) *Cicer arietinum* (Chickpeas)(j) *Launaea procumbens* (Jangi gobi)(k) *Spinacia oleracea* (Spinach)(l) *Coriandrum sativum* (Coriander)

Figure 2. Selected plant samples (g-l) of the study area.

optical emission spectrometry (Agilent 700 Series ICP-OES) for the second sampling, following APHA (2005) protocols. Plant specimens were collected from areas adjacent to the industrial sites and stored in clean plastic bags. Species selected for analysis included *Abutilon indicum*, *Aerva pseudotomentosa*, *Citrullus colocynthis*, *Brachiaria ramosa*, *Cucumis lanatus*, *Calotropis procera*, *Cucumis prophetarum*, *Cicer arietinum*, *Coriandrum sativum*, *Launaea procumbens*, *Prosopis juliflora*, and *Spinacia oleracea*. Each plant sample was separated into root, shoot, and leaf components, then dried in a hot air oven. A subsample of 0.5 g to 1.0 g was weighed using Wensler precision balance. Digestion was performed using the same aqua regia method described for soil samples. Heavy metals - As, Cd, Co, Cr, Cu, Fe, Mn, and Ni - were quantified using APHA (2005) standard procedures.

Assessment of metal accumulation in plants

To evaluate the accumulation and mobility of heavy metals within plant tissues, three indices such as bioconcentration factor, translocation factor and enrichment factor were calculated. Bioconcentration Factor (BCF): It indicates the plant's ability to accumulate metals from the surrounding medium (soil or water). It was calculated as follows (Takarina and Pin, 2017):

$$BCF = \frac{\text{Heavy metal in plant}}{\text{Heavy metal in soil}} \quad [1]$$

Translocation Factor (TF): It reflects the efficiency of metal transfer from roots to shoots which is relevant for assessing phytoextraction potential. TF was calculated as follows (Takarina and Pin, 2017):

$$TF = \frac{\text{Heavy metal in plant shoot}}{\text{Heavy metal in plant root}} \quad [2]$$

Enrichment Factor (EF): It is used to determine the degree of metal enrichment in plant tissues relative to soil, aiding in remediation strategy development (Nowrouzi and Pourkhabbaz, 2015):

$$EF = \frac{\text{Heavy metal in plant shoot}}{\text{Heavy metal in soil}} \quad [3]$$

Contamination and risk analysis in soils and plants

To evaluate the contamination status of soils and plants in the study area, several pollution indices were applied. These include the Contamination Factor (CF), Degree of Contamination (CD), Pollution Load Index (PLI), and Potential Ecological Risk Index (E^f). Their formulas and classifications are summarized in Table 2.

Table 2. Contamination and risk analysis parameters.

Parameter	Formula	Classification	Reference
Contamination Factor (CF)	Contamination Factor = Concentration of metal measured (mg/kg) ÷ Background/reference concentration of the metal (mg/kg)	CF <1: Low, CF 1–3: Moderate, CF 3–6: Considerable, CF >6: Very High	Müller (1969); De Vos et al. (2006)
Degree of Contamination (CD)	Degree of Contamination = Sum of all Contamination Factors	CD <6: Low, CD 6–12: Moderate, CD 12–24: Considerable, CD >24: Very High	Müller (1969)
Pollution Load Index (PLI)	PLI = n-th root of the product of all Contamination Factors (CF ₁ × CF ₂ × ... × CF _n), where n is the number of metals studied	PLI <1: Perfection, PLI 1: Baseline, PLI >1: Deterioration	Tomlinson et al. (1980)
Ecological Risk Index (E ^f)	Ecological Risk Index = Contamination Factor × Toxic Response Factor Toxic response factor for As, Cd, Co, Cr, Cu, Mn, Ni, Pb, and Zn are 10, 30, 5, 2, 5, 1, 5, 5, and 1 respectively (Simeon and Friday, 2017).	E ^f <20: Low, E ^f 20–40: Moderate, E ^f 40–80: Considerable, E ^f 80–160: High, E ^f >160: Very High	Hakanson (1980); Protano et al. (2014); Simeon & Friday (2017)

Health risk assessment

Health risk assessment was conducted using the USEPA model to evaluate both non-carcinogenic and carcinogenic risks associated with heavy metal exposure through ingestion, inhalation, and dermal contact. The formulas and classification criteria used in this study are

presented in Table 3.

Spatial Distribution Mapping

Software QGIS v3.10.5 is used for spatial interpolation of heavy metals. Inverse Distance Weighting (IDW) method generates continuous distribution maps.

Table 3. *Health risk assessment parameters*

Parameter	Formula	Classification	Reference
	$ADD \text{ (Ingestion)} = (\text{Heavy Metal Concentration} \times \text{Ingestion Rate} \times \text{Exposure Frequency} \times \text{Exposure Duration}) \div (\text{Body Weight} \times \text{Averaging Time})$	-	USEPA (2006, 2008, 2014); Rabin et al. (2022)
Average Daily Dose (ADD)	$ADD \text{ (Inhalation)} = (\text{Heavy Metal Concentration} \times \text{Inhalation Rate} \times \text{Exposure Frequency} \times \text{Exposure Duration}) \div (\text{Particle Emission Factor} \times \text{Body Weight} \times \text{Averaging Time})$	-	USEPA (2006, 2008)
	$ADD \text{ (Dermal)} = (\text{Heavy Metal Concentration} \times \text{Skin Surface Area} \times \text{Skin Adherence Factor} \times \text{Dermal Absorption Factor} \times \text{Exposure Frequency} \times \text{Exposure Duration} \times 10^{-6}) \div (\text{Body Weight} \times \text{Averaging Time})$	-	USEPA (2006, 2008)
Hazard Quotient (HQ)	$HQ = \text{Average Daily Dose} \div \text{Reference Dose}$	$HQ < 1: \text{No risk}; HQ > 1: \text{Potential health risk}$	Bai et al. (2021)
Hazard Index (HI)	$HI = \text{Sum of Hazard Quotients from all exposure routes}$	$HI < 1: \text{Safe}; HI > 1: \text{Adverse health effects}$	Bai et al. (2021)
Combined Hazard Index (CHI)	$CHI = \text{Sum of Hazard Indices for all metals}$	-	Bai et al. (2021)
Cancer Risk (CR)	$CR = \text{Average Daily Dose} \times \text{Slope Factor}$	Acceptable: $(10^{-6} \text{ to } 10^{-4})$; Unacceptable: $> 10^{-4}$	USEPA (2007); Pan et al. (2019); Oni et al. (2022)
Cumulative Cancer Risk Index (CRI)	$CRI = \text{Sum of Cancer Risks from ingestion, inhalation, and dermal exposure}$	Acceptable: $(10^{-6} \text{ to } 10^{-4})$; Unacceptable: $> 10^{-4}$	Das et al. (2022)

Results and Discussion

Heavy Metal Contamination in Polluted Soils

The polluted soils of Bikaner city exhibited significant contamination with heavy metals, reflecting both geogenic and anthropogenic influences (Table 4). The concentrations of arsenic (As) and cadmium (Cd) exceeded the permissible limits set by FAO (2007), indicating persistent pollution from industrial activities. The maximum permissible limits in soil (mg/kg) for As, Cd, Cr, Ni, Zn, Cu, Pb, and Mn are 1.0, 1.0, 100, 100, 150, 200, 200, and 1800 (FAO, 2007). While this information is not available for Co and Fe. Arsenic le-

vels were highest in Rani Bazar (7.74 mg/kg, 2019), far surpassing the FAO threshold of 1 mg/kg. Similar findings were reported by Chauhan and Mathur (2020), who attributed elevated As levels in Jaipur's industrial soils to untreated effluents from ceramic and marble industries. Likewise, cadmium concentrations peaked in Karni (4.50 mg/kg, 2020), likely due to discharges from woollen and gypsum industries. Giri et al. (2022) observed even higher Cd levels in Pali's textile zones (up to 454.75 mg/kg), underscoring the widespread nature of industrial Cd pollution in Rajasthan. Iron (Fe) concentrations showed extreme variability, with Rani Bazar recording 2981 mg/kg

Table 4. Heavy metals contents (mg/kg) in soils

Site	Year	As	Cd	Co	Cr	Cu	Fe	Mn	Ni	Pb	Zn
Bichhwal industrial area	2019	7.72	3.36	5.54	14.32	15.7	2580	36	21.52	13.86	41.52
	2020	0	4.47	5.3	5.91	5.46	4.45	5.52	5.67	2.16	4.2
	Mean	3.86	3.91	5.42	10.11	10.58	1292.2	20.76	13.59	8.01	22.86
Rani bazar industrial area	2019	7.74	3.88	4.46	13	18.22	2981	46.5	25.66	9.2	106.12
	2020	0	4.02	5.36	5.37	5.38	4.02	5.57	5.5	0	4.25
	Mean	3.87	3.95	4.91	9.18	11.8	1492.5	26.03	15.58	4.6	55.18
Khara industrial area	2019	7.34	3.88	4.2	14.32	17.94	1104	71.8	21.26	8.92	57.8
	2020	0	4.38	5.12	6.06	5.56	4.1	5.53	5.52	2.2	4.27
	Mean	3.67	4.13	4.66	10.19	11.75	554.05	38.66	13.39	5.56	31.03
Karni industrial area	2019	6.44	3.48	4.92	9.12	13.44	1690	60	17.68	5.72	53.72
	2020	0	4.5	4.85	5.76	5.79	3.89	5.68	5.4	0	4.22
	Mean	3.22	3.99	4.88	7.44	9.61	846.94	32.84	11.54	2.86	28.97

in 2019 and a sharp decline in 2020. This fluctuation may reflect seasonal changes in industrial discharge or sampling variability. Other metals such as chromium (Cr), copper (Cu), manganese (Mn), nickel (Ni), lead (Pb), and zinc (Zn) remained within permissible limits but showed elevated concentrations in specific zones, particularly Rani Bazar and Khara. These findings align with studies by Khan et al. (2022), who reported elevated Cu and Zn levels in soils near Jaipur's industrial belt, and Soliman et al. (2022), who highlighted the ecological risks posed by Pb and Ni in the soils of an Egyptian industrial area. Spatial mapping using QGIS and IDW interpolation revealed distinct contamination hotspots across the industrial zones. In 2019, arsenic was most concentrated in sites S1 (Bichhwal) and S2 (Rani bazar), while Cd, Cr, Cu, and Mn were highest in S3 (Khara) (Fig. 3). In 2020, Cd peaked in S4 and S1, while Co, Cr, Pb, Cu, Mn, Fe, Ni, and Zn showed varied spatial dominance across sites (Fig. 4). These spatial trends underscore the need for site-specific remediation strategies and continuous monitoring. Similar spatial heterogeneity has been reported by Kabir et al. (2022) in Bangladesh's industrial soils, where proximity to effluent discharge.

points significantly influenced metal concentrations.

Pollution Indices and Ecological Risk Assessment

Pollution indices provided quantitative insights into contamination severity. Table 5 displays heavy metals contamination factor (CF), degree of contamination (CD), and pollution load index (PLI) in industrial soils. The values of Contamination Factor (CF) and Degree of Contamination (CD) highlighted cadmium and iron as major pollutants. Bichhwal (2019) recorded the highest degree of contamination (659.2), while Rani Bazar (2019) showed elevated Fe (736). The Pollution Load Index (PLI) exceeded 1 in all sites during 2019, indicating pollution, but dropped below 1 in 2020, suggesting possible seasonal dilution or reduced industrial activity (Hossain et al., 2020).

The Potential Ecological Risk Index (PERI) flagged cadmium as a critical threat across all sites, with values far exceeding the threshold of 40 (Table 6). The eco-toxicological profile of Cd, including its high mobility and bioavailability, makes it hazardous. These findings are corroborated by Delgado-Iniesta et al. (2022), who emphasized Cd's role in disrupting soil microbial activity and plant metabolism.

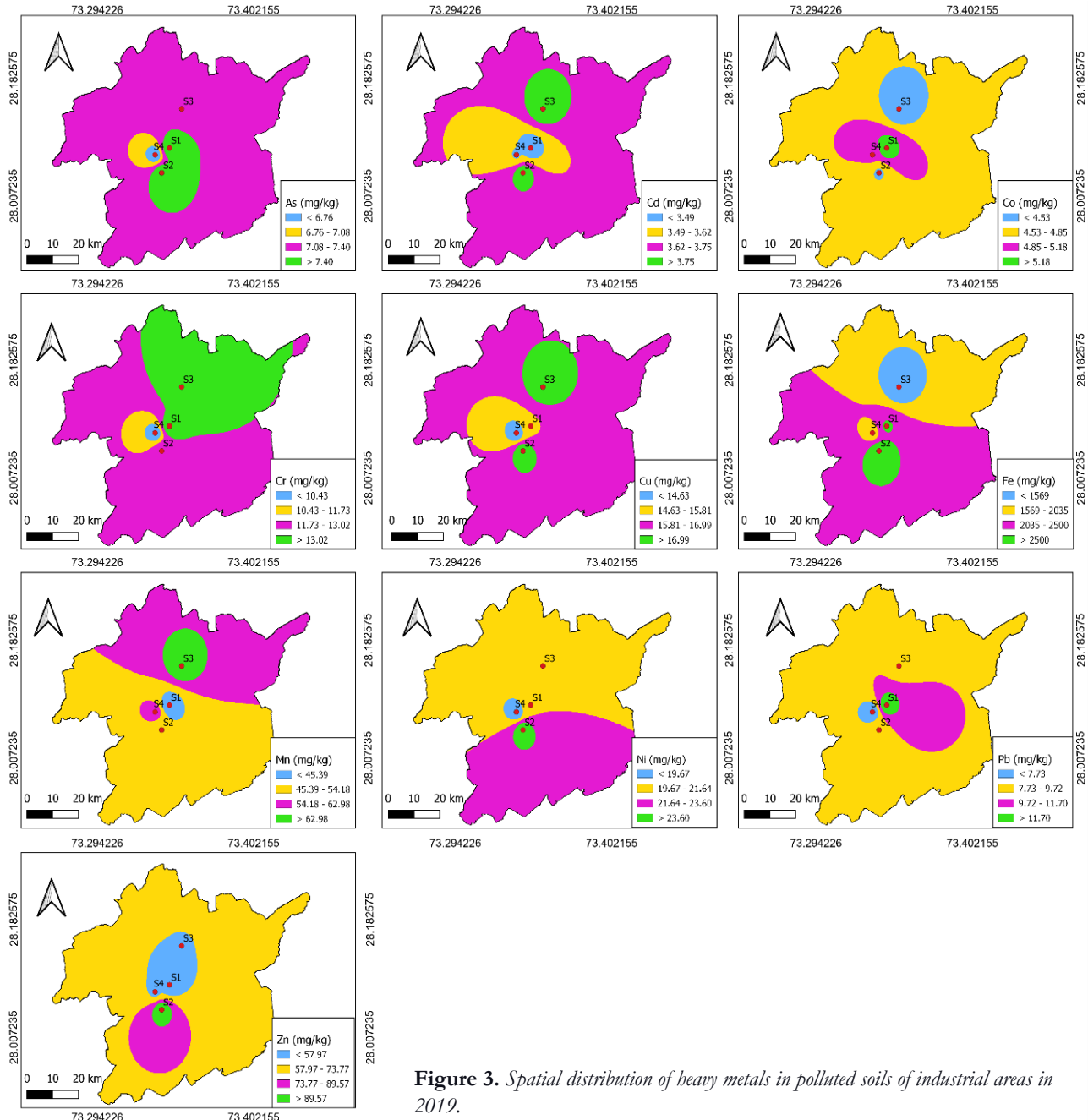


Figure 3. Spatial distribution of heavy metals in polluted soils of industrial areas in 2019.

Table 5. Heavy metals contamination factor (CF), degree of contamination (C_d), and pollution load index (PLI) in polluted soils of industrial areas.

Industrial sites	Year	Contamination factor										C_d	PLI
		As	Cd	Co	Cr	Cu	Fe	Mn	Ni	Pb	Zn		
Bichhwal	2019	0.70	18.06	0.49	0.16	0.91	637	0.04	0.55	0.59	0.67	659.2	1.2
	2020	0.00	24.03	0.47	0.06	0.31	1.09	0.00	0.14	0.09	0.06	26.3	0.419
Rani	2019	0.71	20.86	0.40	0.14	1.05	736	0.06	0.65	0.39	1.73	762	1.34
	2020	0.00	21.61	0.48	0.06	0.31	0.99	0.00	0.13	0.00	0.06	23.6	0.518
Khara	2019	0.67	20.86	0.37	0.16	1.04	272	0.09	0.54	0.38	0.94	297	1.16
	2020	0.00	23.54	0.46	0.06	0.32	1.01	0.00	0.14	0.09	0.06	25.7	0.414
Karni	2019	0.5	18.7	0.44	0.10	0.78	417	0.08	0.45	0.2	0.87	439	1.00
	2020	0.00	24.1	0.43	0.06	0.33	0.96	0.0	0.13	0.00	0.06	26.2	0.521

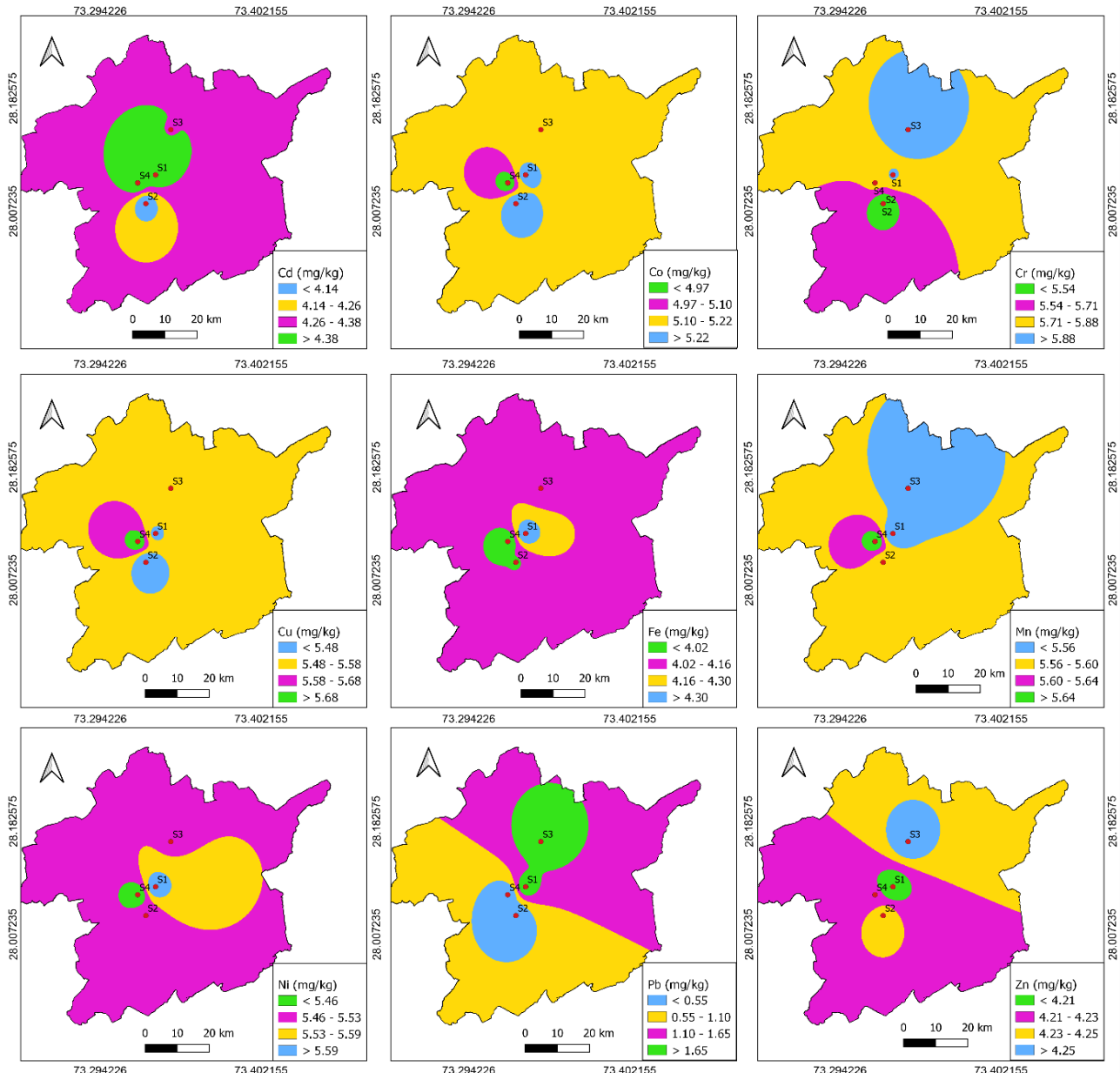


Figure 4. Spatial distribution of heavy metals in polluted soils of industrial areas in 2020.

Table 6. Potential ecological risk index (PERI) in polluted soils of industrial areas.

Industrial sites	Year	As	Cd	Co	Cr	Cu	Fe	Mn	Ni	Pb	Zn
Bichhwal	2019	7.08	541.93	2.49	0.33	4.56	ND	0.04	2.75	2.97	0.67
	2020	0	720.96	2.38	0.13	1.58	ND	0.00	0.72	0.46	0.06
Rani	2019	7.10	625.80	2.00	0.29	5.29	ND	0.06	3.28	1.97	1.73
	2020	0	648.38	2.41	0.12	1.56	ND	0.00	0.69	0	0.06
Khara	2019	6.73	625.80	1.89	0.33	5.21	ND	0.09	2.71	1.91	0.94
	2020	0	706.45	2.30	0.13	1.61	ND	0.00	0.70	0.47	0.06
Karni	2019	5.90	561.29	2.21	0.21	3.90	ND	0.08	2.26	1.22	0.87
	2020	0	725.80	2.18	0.13	1.68	ND	0.00	0.69	0	0.06 7

Phytoremediation potential of native plants

Twelve native plant species were evaluated for their ability to accumulate and translocate heavy metals. Their phytoremediation potential is illustrated in Table 7. Most species demonstrated multi-metal accumulation, with some acting as hyperaccumulators and others as phytostabilizers or excluders. *Citrullus colocynthis* was the only species capable of hyperaccumulating all ten metals in 2019, making it a promising candidate for phytoremediation. *Cicer arietinum* and *Aerva pseudotomentosa* showed high accumulation of Fe, Cd, and Pb in

2020. *Brachiaria ramosa* and *Coriandrum sativum* were effective phytostabilizers for Cr and Mn, while *Spinacia oleracea*, *Prosopis juliflora*, and *Abutilon indicum* acted as excluders for As, Co, and Ni. These roles were confirmed through Bioconcentration Factor (BCF), Translocation Factor (TF), and Enrichment Factor (EF) analyses. Several species showed BCF and TF > 1 , qualifying them as candidates for phytoextraction. These findings align with Soliman et al. (2022), who reported similar phytoremediation potential in *Amaranthus* sp. and *Helianthus annuus* under industrial stress.

Table 7. Phytoremediation potential of native plants in industrial soils

Plants	Hyperaccumulator	Phytostabilizer	Excluder
<i>Brachiaria ramosa</i> (Bichhwal, 2019)	As, Cd, Co, Cr, Cu, Ni, Mn, Pb, Zn	-	-
<i>Abutilon indicum</i> (Bichhwal, 2019)	As, Cr, Cd, Co, Cu, Ni, Mn, Pb, Zn	-	-
<i>Prosopis juliflora</i> (Bichhwal, 2019)	As, Cd, Cr, Co, Cu, Ni, Pb, Zn	-	-
<i>Citrullus colocynthis</i> (Rani Bazar, 2019)	As, Cd, Co, Cr, Cu, Fe, Mn, Ni, Pb, Zn	-	-
<i>Brachiaria ramosa</i> (Rani Bazar, 2019)	As, Cd, Co, Cu, Mn Ni, Pb, Zn	Cr	-
<i>Cucumis lanatus</i> (Rani Bazar, 2019)	As, Cd, Co, Cu, Mn Ni, Pb, Zn	Cr	-
<i>Calotropis procera</i> (Khara, 2019)	As, Cd, Cr, Co, Cu, Ni, Pb, Zn	-	-
<i>Cucumis proferitum</i> (Khara, 2019)	As, Cr, Cd, Co, Cu, Ni, Zn	-	-
<i>Citrullus colocynthis</i> (Khara, 2019)	As, Cr, Cd, Cu, Co, Ni, Pb, Zn	-	-
<i>Abutilon indicum</i> (Karni, 2019)	As, Co, Cr, Cd, Cu, Ni, Pb, Zn	-	Fe and Mn
<i>Cucumis lanatus</i> (Karni, 2019)	As, Cr, Cd, Cu, Co, Ni, Pb, Zn	-	-
<i>Aerva pseudotomentosa</i> (Karni, 2019)	As, Cd, Co, Cr, Cu, Fe, Mn, Ni, Pb	Mn	-
<i>Brachiaria ramosa</i> (Bichhwal, 2020)	Cd, Cu, Cr, Fe, Pb, Mn, Zn	-	As, Co, Ni
<i>Abutilon indicum</i> (Bichhwal, 2020)	Cd, Cu, Cr, Fe, Pb, Mn, Zn	-	As, Co, Ni
<i>Prosopis juliflora</i> (Bichhwal, 2020)	Cd, Cu, Cr, Fe, Pb, Mn, Zn	-	As, Co, Ni
<i>Spinacia oleracea</i> (Rani, 2020)	Cd, Cu, Cr, Fe, Pb, Mn, Zn	-	As, Co, Ni
<i>Brachiaria ramosa</i> (Rani, 2020)	Cd, Cu, Fe, Zn	Mn	As, Co, Cr, Ni
<i>Coriandrum sativum</i> (Rani, 2020)	Cd, Cr, Cu, Fe, Zn	Mn	As, Co, Ni
<i>Calotropis procera</i> (Khara, 2020)	Cd, Cr, Cu, Fe, Mn, Pb, Zn	-	As, Co, Cr
<i>Launaea procumbens</i> (Khara, 2020)	Cd, Cu, Cr, Mn, Fe, Pb, Zn	-	As, Co, Ni
<i>Aerva pseudotomentosa</i> (Khara, 2020)	Cr, Fe, Cu, Ni, Mn, Pb, Zn	-	As, Cd, Co
<i>Abutilon indicum</i> (Karni, 2020)	Cu, Fe, Mn, Zn	-	As, Cd, Co Cr, Ni
<i>Cicer arietinum</i> (Karni, 2020)	Cd, Cu, Cr, Mn, Fe, Ni, Zn	-	As, Co
<i>Aerva pseudotomentosa</i> (Karni, 2020)	Cd, Cu, Cr, Mn, Fe, Zn, Ni	Co	As, Pb

Human Health Risk Assessment

Noncarcinogenic risk.

Children were more vulnerable than adults, particularly via ingestion and dermal contact. Mn and Pb posed significant risks, with Hazard Quotient (HQ) values exceeding safe limits. In 2019, the highest cumulative hazard index (cHI) was

found in children from Khara (1.33), while in 2020, Karni children also exceeded the threshold (1.14) as shown in Table 8. Dermal exposure to Mn and ingestion of Pb were the dominant pathways. These findings are consistent with Li et al. (2018), who emphasized children's heightened susceptibility due to behavioral and physiological factors.

Table 8. Cumulative hazard indices (cHI) of heavy metal contaminated industrial soils.

Industrial area	Year	Target group	HI _{ingestion}	HI _{inhalation}	HI _{dermal}	cHI
Bichhwal	2019	Children	0.24830653	6.6156E-05	0.7053204	0.9536931
		Adult	0.03117097	3.8743E-05	0.1382810	0.1694908
	2020	Children	0.04795525	3.1004E-05	0.2899210	0.3379072
		Adult	0.01891200	1.1998E-05	0.0545916	0.0735156
Rani Bazar	2019	Children	0.24538388	6.5212E-05	0.7938252	1.0392743
		Adult	0.03182141	3.4339E-05	0.1616368	0.1934926
	2020	Children	0.04032406	2.8033E-05	0.2859152	0.3262672
		Adult	0.01411180	1.0838E-05	0.0538507	0.0679734
Khara	2019	Children	0.23907605	7.0461E-05	1.0952089	1.3343554
		Adult	0.02104678	3.65E-05	0.2127394	2.34E-01
	2020	Children	0.04769851	3.1101E-05	0.2849482	0.3326778
		Adult	0.01901184	1.2294E-05	0.0536708	0.0726950
Karni	2019	Children	0.19945742	5.1897E-05	0.9417327	1.1412420
		Adult	0.01790048	2.5178E-05	0.1834275	0.2013532
	2020	Children	0.04392827	0.82082945	0.2775991	1.1423569
		Adult	0.01421175	1.1646E-05	0.0542329	0.0684563

Carcinogenic risk.

Cadmium and nickel emerged as the most hazardous metals. In 2019, Rani Bazar adults had a CRI of 1.6×10^{-4} , indicating elevated cancer risk (Table 9). In plants, *Cicer arietinum* and *Coriandrum sativum* showed the highest CR values, with Cd being the dominant contributor. These findings highlight the urgent need for public health interventions and safer agricultural practices. Sonone et al. (2020) similarly reported elevated cancer risks from Cd and Ni in contaminated crop zones of Maharashtra.

These findings highlight the urgent need for public health interventions and safer agricultural practices. Sonone et al. (2020) similarly reported elevated cancer risks from Cd and Ni in contaminated crop zones of Maharashtra.

Year	Target groups	Carcinogenic Risk Index			
		Bichhwal	Rani Bazar	Khara	Karni
2019	Children	2.71E-05	2.86E-05	2.7E-05	2.15E-05
	Adult	1.48E-05	0.000163	1.47E-05	1.21E-05
2020	Children	9.95E-06	9.12E-06	9.87E-06	9.74E-06
	Adult	2.28E-05	2.54E-05	2.24E-05	1.97E-05

Table 9
Carcinogenic risk index of heavy metal contaminated industrial soils.

Conclusions

The rapid industrial expansion in Bikaner, while economically beneficial, has led to significant environmental degradation, particularly through heavy metal contamination in wastewater, soil, and vegetation. This study provides a comprehensive assessment of ten heavy metals - As, Cd, Co, Cr, Cu, Fe, Mn, Ni, Pb, and Zn - across four major industrial zones: Bichhwal, Rani Bazar, Khara, and Karni. Key findings reveal that cad-

mium and arsenic frequently exceed permissible limits, especially in Karni and Rani Bazar, posing serious ecological and health risks. Iron concentrations were notably high in Rani Bazar, likely due to effluents from woolen industries. Spatial and temporal analyses show a marked increase in contamination levels from 2019 to 2020, with Karni emerging as the most affected zone. The study also highlights the phytoremediation potential of native plant species. Several plants, includ-

ding *Citrullus colocynthis*, *Cicer arietinum*, and *Aerva pseudotomentosa*, demonstrated strong hyperaccumulation capabilities, while others like *Spinacia oleracea* and *Abutilon indicum* acted as metal excluders or phytostabilizers. These findings underscore the dual role of vegetation—as both a victim of contamination and a tool for remediation. Health risk assessments indicate that children are particularly vulnerable, with hazard quotients and carcinogenic risk indices exceeding safe thresholds for multiple metals. Cd and Pb pose the greatest threat, especially through ingestion and dermal exposure. The presence of these metals in edible plants raises urgent concerns about food safety and public health. In summary, the unchecked discharge of industrial effluents has created a complex web of contamination that affects soil fertility, plant health, and human well-being. Immediate interventions - such as stricter regulatory enforcement, continuous monitoring, and the adoption of phytoremediation strategies - are essential to mitigate these risks and promote sustainable industrial practices in Bikaner.

Acknowledgements

The authors would like to thank the Department of Environmental Science, Maharaja Ganga Singh University, Bikaner for sample analysis.

References

ADEDIRAN A., LEMOUGNA P.N., YLINIEMI J., TANSKANEN P., KINNUNEN P., RONING J., ILLIKAINEN M. (2021) Recycling glass wool as a fluxing agent in the production of clay- and waste-based ceramics. *Journal of Cleaner Production*, 289:125673.
<https://doi.org/10.1016/j.jclepro.2020.125673>

ALI H., KHAN E., SAJAD M.A. (2019) Phytoremediation of heavy metals: concepts and applications. *Chemosphere*, 91(7):869–881.
<https://doi.org/10.1016/j.chemosphere.2019.01.075>

APHA. (2005) Standard methods for the examination of water and waste water. 21st Edition, American Public Health Association, American Water Works Association, Water Environment Federation.

AYANGBENRO A.S., BABALOLA O.O. (2017) A new strategy for heavy metal polluted environments: A review of microbial biosorbents. *International Journal of Environmental Research and Public Health*, 14(1):94.
<https://doi.org/10.3390/ijerph14010094>

BAKSHI A., PANDEY R., SHARMA S. (2018) Heavy metal pollution of soil and its phytoremediation. In: Kumar V., Kumar P., Sharma S. (Eds), *Environmental Pollution and Remediation*. Springer, Singapore, pp: 1–24.

BAI L., ZHANG Y., LIU Q., WANG J. (2021) Health risk assessment of heavy metals in urban soils and vegetables: A case study from China. *Environmental Pollution*, 268:115944. <https://doi.org/10.1016/j.envpol.2020.115944>

CHAUHAN R., MATHUR R. (2020) Assessment of arsenic contamination in industrial soils of Jaipur. *Environmental Monitoring and Assessment*, 192(3):145.
<https://doi.org/10.1007/s10661-020-8123-4>

CUI X., LIU Y., ZHANG Y., WANG L. (2022) Heavy metal pollution in soil and its health risk assessment in industrial areas of China. *Environmental Science and Pollution Research*, 29(5):6543–6556.
<https://doi.org/10.1007/s11356-021-16023-3>

DAS S., MONDAL N.C., RAHMAN A. (2022) Cumulative cancer risk assessment of heavy metals in groundwater of semi-arid regions of Rajasthan, India. *Environmental Geochemistry and Health*, 44(6): 2183–2198.
<https://doi.org/10.1007/s10653-021-01045-9>

DELAGO-INIESTA M., GARCIA-GOMEZ C., FERNANDEZ J.M. (2022) Cadmium toxicity in soil microbial communities: A review. *Ecotoxicology and Environmental Safety*, 231:113174.
<https://doi.org/10.1016/j.ecoenv.2022.113174>

DE VOS W., TURETTE R., VAN DER WEELE J. (2006) Soil contamination assessment using CF indices. *Environmental Geology*, 50(4): 465–472.

FAO. (2007) Guidelines for soil quality standards. Food and Agriculture Organization, Rome.

GIRI S., SHARMA P., SINGH R. (2022) Heavy metal contamination in Pali's textile zones: A geochemical perspective. *Journal of Environmental Management*, 305: 114234. <https://doi.org/10.1016/j.jenvman.2022.114234>

HAKANSON L. (1980) An ecological risk index for aquatic pollution control. A sedimentological approach. *Water Research*, 14(8):975–1001.

HOSSAIN M.B., ISLAM M.N., ALAM M.S., HOSSEN M.Z. (2020) Seasonal variation of heavy metal concentrations in farm soils of Sreepur Industrial Area of Gazipur, Bangladesh: Pollution level assessment. *American Journal of Environmental Sciences*, 16(4):68–78.
<https://doi.org/10.3844/ajessp.2020.68.78>

KABIR M.H., RAHMAN M.S., ISLAM M.T. (2022) Spatial heterogeneity of heavy metals in industrial soils of Bangladesh. *Environmental Geochemistry and Health*, 44(3):1123–1138.
<https://doi.org/10.1007/s10653-021-01045-9>

KHAN M.A., SINGH R., YADAV V. (2022) Heavy metal contamination in Jaipur's industrial belt: A spatial analysis. *Journal of Hazardous Materials*, 429:128314.
<https://doi.org/10.1016/j.jhazmat.2022.128314>

KUNWAR R., JAIN S. (2022) Phytoremediation potential of native desert plants in Rajasthan. *Journal of Environmental Biology*, 43(2): 215–222.

LI Y., ZHANG X., WANG J. (2018) Health risk assessment of heavy metals in children: A case study from China. *Environmental Pollution*, 243:1407–1416.
<https://doi.org/10.1016/j.envpol.2018.09.032>

MÜLLER H. (1969) Index of geoaccumulation in sediments of the Rhine River. *GeoJournal*, 2(3):108–118.

NOWROUZI M., POURKHABBAZ H.R. (2015) Phytoremediation potential of native plants in industrial zones. *Ecotoxicology*, 24(3): 595–604.

ONI O., SIMEON O., ADEBAYO A. (2022) Carcinogenic and non-carcinogenic health risk assessment of heavy metals in contaminated soils. *Environmental Monitoring and Assessment*, 194(3):145.
<https://doi.org/10.1007/s10661-022-09876-3>

PAN X., LIU Y., ZHANG W., WANG L. (2019) Human health risk assessment of heavy metals in agricultural soils: A case study from China. *Ecotoxicology and Environmental Safety*, 180: 549–556.
<https://doi.org/10.1016/j.ecoenv.2019.05.041>

PROTANO G., GIAMPIETRO F., SPERANZA A., FABIETTI G. (2014) Heavy metal concentrations in soils and mosses from urban and rural areas of central Italy: Evaluation of pollution and ecological risk. *Environmental Science and Pollution Research*, 21(5): 3305–3316.
<https://doi.org/10.1007/s11356-013-2313-3>

SHARMA R.K., NAGPAL A.K. (2018) Soil contamination with heavy metals and its impact on human health. *Environmental Science and Pollution Research*, 25(3): 2345–2356. <https://doi.org/10.1007/s11356-017-0566-6>

SIMEON O., FRIDAY O. (2017) Human health risk assessment of heavy metals in contaminated soils. *Journal of Environmental Science and Health*, 52(9): 765–774.

SINGH R., YADAV V. (2014) Impact of industrial effluents on water quality in urban India. *Journal of Environmental Research and Development*, 9(2): 345–352.

SOLIMAN N.F., MOHAMED A.A., HASSAN M.A. (2022) Ecological risk of heavy metals in Egyptian industrial soils and phytoremediation potential of native plants. *Environmental Science and Pollution Research*, 29(5):6543–6556. <https://doi.org/10.1007/s11356-021-16023-3>

SONONE S.S., JADHAV S.S., PATIL S.S. (2020) Carcinogenic risk from cadmium and nickel in contaminated crop zones of Maharashtra. *Environmental Monitoring and Assessment*, 192(4):215.
<https://doi.org/10.1007/s10661-020-8201-7>

TAKARINA N.D., PIN T.G. (2017) Bioconcentration Factor (BCF) and Translocation Factor (TF) of Heavy Metals in Mangrove Trees of Blanakan Fish Farm. *Makara Journal of Science*, 21(2):77–81.
<https://doi.org/10.7454/mss.v21i2.7308>

TANWAR V., DESWAL M., KHYALIA P., MEHLA S.K., DALAL H. (2019) Phytoremediation of heavy metals using *Brassica juncea* and *Prosopis juliflora*. *Environmental Sustainability*, 2(3): 215–223.

TOMLINSON D.L., WILSON J.G., HARRIS C.R., JEFFREY D.W. (1980) Problems in the assessment of heavy-metal levels in estuaries and the formation of a pollution index. *Helgoländer Meeresuntersuchungen*, 33(1–4):566–575.

USEPA. (2006) Risk Assessment Guidance for Superfund Volume I: Human Health Evaluation Manual (Part E, Supplemental Guidance for Dermal Risk Assessment). EPA/540/R/99/005, U.S. Environmental Protection Agency, Washington, DC.

USEPA. (2007) Framework for Metals Risk Assessment. EPA 120/R-07/001, U.S. Environmental Protection Agency, Washington, DC.

USEPA. (2008) Exposure Factors Handbook. EPA/600/R-09/052F, U.S. Environmental Protection Agency, Washington, DC.

USEPA. (2014) Human Health Risk Assessment Protocol for Hazardous Waste Combustion Facilities. EPA530-R-05-006, U.S. Environmental Protection Agency, Washington, DC.

YANG Y., LIU X., ZHANG Y., ZHOU J. (2018) Sources and health risks of heavy metals in urban soils of China. *Ecotoxicology and Environmental Safety*, 156: 1–8. <https://doi.org/10.1016/j.ecoenv.2018.03.017>

ZAYNAB M., FATIMA M., ABBAS S., SHAHZAD K., AHMAD A., ZAFAR M.H., IQBAL M. (2020) Role of secondary metabolites in plant defense against pathogens. *Microbial Pathogenesis*, 137:1